EMS602U Simulation Tools in Engineering Analysis and Design
Inviscid Flow over a Compressor Stator Blade
CFD Laboratory Report

Group 70
Riyadh Miah 200383163
Joost Hubbard 210372773
Safwan Bin Ahmed 210183881
Mohamed Ghandoura 200513162

Abstract

The aim of the computational fluid dynamics laboratory was to evaluate the effect of mesh refinement and order of accuracy upon the simulation of inviscid flow over a compressor stator blade and simulation outputs. The simulation was completed using STAR CCM+ to simulate the flow over a two-dimensional profile of a blade; this could be extrapolated to the remainder of the blades due to their symmetrical placement within the compressor. As a result, it was established that the most accurate sequence simulation, in terms of static and total pressure coefficients in addition to force coefficients, was the fine second order mesh. With the increase of both refinement and order, the amount of error is reduced when compared to the theoretical values, and the simulation becomes smoother and more stable. It was also found that local mesh refinement can result in similar solutions at lower element counts and thus less computational demands.

Table of Contents

1. Introduction

The computational fluid dynamics laboratory aimed to analyse and optimise incompressible, inviscid flow over a two-dimensional stator mesh, concentrating on the influence of mesh refinement and the order of accuracy. Across the report, a myriad of flow features will be investigated and their relationship to mesh properties compared. To ensure accurate discussion of results, an initial understanding of the simulations and parameters used is paramount. The areas of interest in relation to the simulation setup include viscous flow, flow separation, boundary conditions, artificial viscosity, mesh resolution, residuals, and mesh convergence.

When approaching simulation of fluids, an understanding of how viscosity acts within a flow is key. Viscous flow is flow in which viscosity is accounted for, representing the internal resistance of the fluid to motion. This internal resistance manifests due to friction between pairs of particles as well as between particles and a surface. When applied to a flow, viscosity can cause a velocity gradient between a surface and the freestream commonly referred to as the boundary layer. Furthermore, viscous interaction between particles accounts for drag forces in the flow leading to flow features such as wake. In cases where the boundary layer can no longer follow a surface, the flow detaches and beings to flow separately. This commonly occurs due to an adverse pressure gradient, leading to boundary layer flow reversal and ultimately the separation of the boundary layer from the surface. When flow separates, it typically forms vortices leading to reduced lift and an increase in pressure drag – caused by the large pressure difference between the front and rear surfaces of the subject.

In the case of our simulations, inviscid flow (flow which negates viscosity) will be used to reduce computational impact. This means that the air will act as an ideal fluid with constant density and no shear stress. Due to this, the formation of the boundary layer cannot occur on the surface of the blade and should not be present in accurate simulation.

As a result of this, artificial viscosity is added to the simulation. Artificial viscosity or dissipation is an error added to inviscid flow simulations to ensure stability of the numerical model. By accounting for the lack of physical viscosity, numerical simulations can still be conducted, and the chosen discretisation can remain stable. The artificial viscosity required for a simulation remain stable can vary based on a few factors, namely the order of the scheme as well as mesh refinement and quality. As the order of a scheme increases, the amount of artificial viscosity required diminishes. Artificial viscosity can also be minimised by refining the mesh around points of high-pressure gradient as well as by improving mesh quality. Minimising the added viscosity reduces error and ensures the simulation is as accurate as possible.

Additional parameters set to facilitate the simulations are called boundary conditions. Boundary conditions are applied to simulations to control what occurs at the edge of the test regions during CFD simulations. Within a typical CFD simulation, inlet and wall boundary conditions are set. The inlet condition sets the mass flow rate into the system while the wall imposes a restriction on the flow - either allowing or preventing flow through the surface. Within an advection simulation, the outlet does not require a boundary condition as, due to the up winding across the flow, the physically correct flux is calculated at the outlet based on the inlet condition. Incorrectly setup boundary conditions (such as an outlet condition inconsistent with up-winded flux calculations) can lead to failure.

Across the lab, the meshes used vary in resolution, refining from coarse through to fine. The refinement of a CFD simulation mesh refers to increasing the number of elements being modelled across a test case. Typically, an increased mesh resolution can provide more accurate representation of small-scale flow features as well as promote convergence in output results; error is also minimised as previously mentioned. Unfortunately, higher mesh resolution comes with an increased computational demand and as such a middle ground must be found. This middle ground can be achieved using localised mesh refinement reducing computational cost while still maintaining accuracy around integral flow features.

When running the simulations residuals were monitored. The residuals of a simulation represent the disparity between computed values and those predicted by use of the numerical method. When residuals are minimised, this means convergence has been reached. Convergence is the point at which error is diminished – giving accurate and consistent values. After convergence, mesh refinement has no impact on values attained, instead just increasing the speed at which convergence is reached. Because of this, it can be determined high residuals are an indicator of numerical instability or inadequate element sizing.

1.1 Setup Parameters

To conduct the CFD simulations, initial setup was required for each mesh case – allowing for the standardisation of each simulation for later comparison.

1. The physics model was set up to follow a 'simple' discretisation scheme assuming segregated flow. The accuracy of the discretisation is determined by the order, either first or second. For this lab, both cases must be run for each mesh.

2. The flow was set to incompressible and inviscid – ensuring a constant density and the negation of viscous effects.

3. The gas within the simulation was set to have a density of 1.225 kg/m^3. This ensures it is consistent with air at atmospheric pressure.

4. The initial conditions were set for both pressure and velocity. The pressure was set at 0 Pa while the x-velocity component was set at 10 m/s. The y and z components of velocity were set to remain at 0 m/s.

5. A reference value was set for pressure as atmospheric pressure (0 Pa). Reference density is set to constant.

6. The boundary conditions associated with the simulation were set for the walls, inlet, and outlet. The wall is set to be impenetrable by the fluid; the inlet is set to have a whirl angle of -38 degrees with a total pressure of 860 Pa and the outlet is set to pressure outlet – imposing a back pressure.

7. The lower and shadow period boundaries are set to 'periodic' and imposed on the two interfaces. This reflects simulation of the 15 other blades.

8. Reports are created for axial and circumferential force coefficients as well as total element number.

9. Residuals plot is created alongside plots for the total and static pressure coefficients along both the upper and lower surfaces of the blade.

10. Contour plots are created for the velocity magnitude, ensuring a constant legend and colour scheme across all plots created.

11. Stopping criteria are implemented. Maximum steps are set to 1000 and criteria are set based on each meshes convergence values based on continuity and momentum thresholds.

2. Results

The results section of this report covers qualitative and quantitative investigation into the flow parameters discussed previously. Displayed in the appendix are all visual and graphical outputs from STAR-CCM+ for every mesh refinement and order of accuracy.

2.1 Effect of Mesh Refinement and 2nd Order Accuracy

After completion of the simulation, the flow parameters of interest can be analysed. The first point of interest, velocity magnitude, can be seen displayed as a contour plot in Table 1 for each sequence mesh and order. When comparing the effect of an increased order of accuracy and mesh resolution, the contours allow for qualitative analysis.

Focusing first on the boundary layer over the surfaces of the blade, both mesh resolution and order of accuracy are found to have a large effect. As the resolution of the mesh increases, the number of visible velocity contours appears to decrease, and those remaining group closer to the upper surface. The smaller number of velocity contours indicates a lack of velocity gradient and thus the removal of the boundary layer from high resolution simulations. A similar effect occurs when increasing the order, pushing the existing velocity contours closer

to the surface, further reducing the velocity profile over the high-pressure surface of the blade. This phenomena can be explained by the fact that the flow simulation is treated as inviscid – meaning that the lack of viscosity in the flow should negate the existence of the boundary layer. As a result of this, any contours that suggest a boundary layer in the contour plots are found because of artificial viscosity and are in fact a simulation error (Müller, 2015). This error is reduced at higher orders of accuracy and mesh resolution, as demonstrated by the contour plots, leaving the second order fine mesh as the most accurate simulation.

Following this, analysis of the stagnation points, on the leading and trailing edge, can be conducted. To identity key differences in the effect of resolution, the coarse and fine second order meshes are compared. Firstly, the smoothness of the velocity contours is seen to improve drastically with an increase in mesh refinement – removing perturbations from the flow. This can be seen as an increase in accuracy since the flow is inviscid and as such should only be impacted by the high-pressure gradient, ignoring viscous forces from the surrounding flow. Due to this, it can be determined that the fine mesh is the most accurate. In terms of the order of accuracy, improvements can also be identified with increase. Comparing all three first order sequence meshes against their second order counterparts; a drastic change can be identified near the trailing edge. As the order increases, the velocity gradients become more localised to the point of high pressure, reducing the visible wake. This is particularly clear in the fine mesh due to the removal of perturbations allowing the wake to form a circular, local velocity gradient - as would be expected for inviscid flow.

Across the lower surface of the blade, high velocities are recorded indicating very low pressure. When the order of accuracy of the simulation increases, the velocity contours in this region become more defined and smoother, suggesting a greater accuracy velocity gradient. Increasing the resolution of the mesh used seems to localise the velocity gradient. Using Graph 2, the region can be further investigated in terms of static pressure. When identifying the suction peak, the negative maximum of pressure coefficient is reached by the fine second order mesh closely followed by the medium fine mesh. This suggests that they key factor in determining accuracy in terms of static pressure is order of accuracy.

Across the blade, Graph 1 displays the pressure gradient for each mesh refinement and order of accuracy simulated. Since the flow is inviscid, the total pressure across a streamline should remain constant (Benson, 2023) and as such the coefficient should remain near 1.15 (the theoretical total pressure coefficient calculated in Section 2.3). Using this knowledge, it can be established that a fine, second order simulation is the most accurate. This is because both its upper and lower surfaces maintain a total pressure coefficient close to one. One explanation for this, is the reduction of artificial viscosity at higher orders combined with a finer mesh to provide stability. This stability reduces perturbations in the data; smoothness in the flow is seen to grown with mesh refinement. This is shown as shown by the peak at the start of the coarse, second order case which seems to diminish at high resolutions.

Overall, it can be established that both the order of accuracy and level of mesh refinement play key roles in simulation accuracy. With the increase of both, the amount of error (in the form of artificial viscosity) is reduced, and the simulation becomes smoother and more stable.

2.2 Comparison of 'other' with Comparable Sequence Simulation
Within this section, the 'other' and an equivalent sequence simulations are compared determine any similarities or differences. In this case, the comparable sequence mesh is the 'medium' mesh since both have an element count of 15466 – this is displayed in Graph 5. Only the second order simulations are evaluated based on the conclusions gleamed in Section 2.1. At the outset, it can be noted that the element shapes, shown in Table 2, vary between the two mesh types, despite having the same element count. The 'other' mesh contains more varied element shapes and density, particularly round points of high pressure and velocity gradient. This is an indication of local mesh refinement and is worth noting for later discussion.

Initial analysis of the two meshes can be conducted making use of Tables 1 and 2, allowing for analysis of flow features as was conducted in Section 2.1. Focusing first on the suction peak, neither plot appears to represent a significant change, with the velocity contours being essentially identical across both meshes. This similarity is contrasted at the leading and trailing edges, with a large disparity between the meshes. The velocity contours using the 'other' mesh are smooth and localised to the stagnation point – much like what is seen with finer meshes. The medium mesh appears to lack clear definition of pressure regions. This can be explained by

an overshoot in the medium mesh simulation because of added artificial viscosity to stabilise the simulation. This suggests that the other mesh requires less added viscosity for a stable simulation and as such results in less error; this occurs because of local mesh refinement around points of high-pressure gradient.

Numerical analysis of Graphs 3 and 4 provide a means to compare both static and total pressure coefficients along the length of the blade. The total pressure, as discussed in Section 2.1 should be close to theoretical as possible based on simulation parameters – namely the use of inviscid flow. Comparing the medium and 'other' mesh, it is clear the other mesh is more accurate across its length. While the peak at the front stagnation point is still pronounced, the remained of the 'other' pressure coefficients sit far closer to 1.15 (the theoretical total pressure coefficient calculated in Section 2.3) for both the upper and lower surfaces; the medium mesh pressure coefficients sit far below 1.15 at across the length of the blade. Referring to Graph 1, the other mesh is possibly the most accurate mesh available due to its local mesh refinement. The static pressure graphs are almost identical for the medium and other meshes. This is to be expected based upon the minimal differences on the velocity contour plot. The main reason can be explained by the relationship between static pressure and order of accuracy, described by Müller (2015), since both simulations are of the same order and local mesh refinement only covers a small section of the blades surface.

Overall, despite equivalent element count and order of accuracy, it is observed that the 'other' mesh outperforms the medium mesh in terms of simulation accuracy – almost entirely due to local mesh refinement around the blade's stagnation point. The additional refinement reduces the artificial viscosity required to maintain stability ensuring higher performance with equal computational cost.

2.3 Quantitative Comparative of Total Pressure and Force Coefficients

Graph 1 displays the total pressure coefficient (CP) values against the x position along the stator blade. For all the mesh types, there is initially a significant drop in the CP due to the flow hitting the leading edge of the blade, where there is a high rate of change in momentum. At this point, the velocity is zero. The flow then starts moving along the blade's surface, accelerating rapidly until it reaches the suction peak, as shown by the sudden upshoot in Graph 1. The graph then plateaus as the fluid continues moving along the surface of the blade until another upshot and drop in CP, where vortices have occurred.

Comparing the 2nd order sequence meshes, it is seen that they all follow the general trend explained above, with the fine mesh having the largest CP and lowest pressure drop, while the coarse mesh had the smallest CP and most significant pressure drop. The 2nd order other mesh was most comparable to the 2nd order medium mesh, with a slightly higher CP along the graph and a much smaller pressure drop at the leading and trailing edge of the blade. Compared to the fine mesh, the other mesh had a lower CP value along the graph and more significant pressure drops.

To calculate the total pressure, the sum of the dynamic pressure and static pressure must be found. In theory, for this stator blade case, the total pressure should be 860Pa. However, this is not the case, as even with inviscid flow, there is still an artificial viscosity causing a pressure loss in the system.

To calculate the theoretical pressure coefficient, Equation 1 was used:

$$\mathbf{C_P} = \frac{Total\ P}{Dynamic\ P} = \frac{P}{0.5 \times \rho \times v^2} = \frac{860}{0.5 \times 1.225 \times 35^2} = \mathbf{1.15} \qquad \qquad [1]$$

Where P is the total pressure, ρ is the gas density and v is the velocity.

This theoretical CP value was compared with the simulated CP values for each sequence mesh in *Table 3*, where the percentage error was calculated. These tabulated errors were then plotted on *Graph 6* to visualise the magnitude of the errors. As expected, it was seen that the 2nd order fine mesh was the most accurate with respect to the theoretical CP as it had the lowest percentage error of 10.62%. The 1st order coarse mesh was the least accurate, with a percentage error of 39.17%. In general, as the mesh becomes more refined, e.g. from a coarse to a fine mesh, the error of the simulated CP will reduce as finer meshes have more simulated element numbers. This refinement allows for a more accurate identification of small-scale flow features, such as stagnation points. This is also the case for the 1st and 2nd order segregated flow, where the 2nd order is found to have relatively smaller percentage errors.

Graph 5 shows the 2nd order fine mesh with the most elements and the 2nd order coarse mesh with the least elements. The 2nd order medium mesh and the 2nd order other mesh, which are similar in element number, have much fewer elements than the fine mesh but slightly more relatively than coarse mesh. In Graph 7, the fine meshes have the largest coefficient of force with some anomalies. This is apparent for the 2nd order circumferential case, where the medium mesh has a larger coefficient of force (Cf) and for the 2nd order axial case, where the medium mesh has an almost equal Cf. In all cases, excluding the 2nd order circumferential Cf, the coarse mesh has the lowest Cf value. From the graph and the points stated, by increasing the element number for a mesh, more accurate results can be found as the mesh has been more refined. However, for computational modelling, it can cost more and be time-consuming compared to lower element number meshes. The same advantages and disadvantages can be said for using the 2nd order meshes instead of 1st order meshes.

By analysing the behaviour of total and static pressure as well as force, it is implied that the most accurate and best mesh should be the fine mesh. The other mesh is the next best mesh, with the medium mesh closely following behind. The coarse mesh is seen as the least accurate mesh.

3. Summary
To summarise, it is clear from analysis conducted in 2.1, the increase of order of accuracy and resolution lead to more accurate simulation. The results indicate that increasing mesh refinement and order of accuracy results in smoother velocity and pressure profiles, in addition to increased stability. Furthermore, the artificial viscosity is seen to reduce and induce less error, resulting in more accurate simulations.

As a result of these findings the meshes were compared to establish efficacy. It was found that, for sequence meshes, a fine mesh using a second order accuracy scheme was the most optimal. This resulted in a in a much lower error value when compared to theoretical values - 10.62% error. The fine mesh improves the coarse mesh in terms of capturing complicated flow patterns and keeping the overall pressure coefficients close to theoretical values. The increase of order is found to smooth out flow pattens providing smoother flow with reduced artificial viscosity.

The value of local mesh refinement was also made clear by the evaluation of the 'other' mesh in 2.1, providing superior performance at lower computational demand when compared to the medium mesh. Artificial viscosity was reduced in the 'other' mesh; while the medium mesh contained overshoots and a lack of clear characterization of pressure regions, implying limits in capturing important flow properties.

Overall, it can be determined that while simulation can be improved significantly through the increase of mesh refinement or order of accuracy, error and computational demand are perpetual issues. The addition of local mesh refinement around points of high pressure gradient works to resolve computational limits ad reduced numerical addition however issues still persist. As a result, care must be taken when making use of computational flow dynamics simulations to ensure this error is minimised and recognised when it does occur. This can be achieved through analysis of output data to predicted flow features as sis conducted across the repot.

4. References

1. Müller, J. (2015). *Essentials of computational fluid dynamics.* CRC Press.

2. Benson, T. (2023, 12 13). *Bernoulli's Equation.* Retrieved from NASA: https://www.grc.nasa.gov/www/k-12/VirtualAero/BottleRocket/airplane/bern.html

5. Appendix

Table 1 - Velocity magnitude contour plots for each mesh type and order of accuracy.
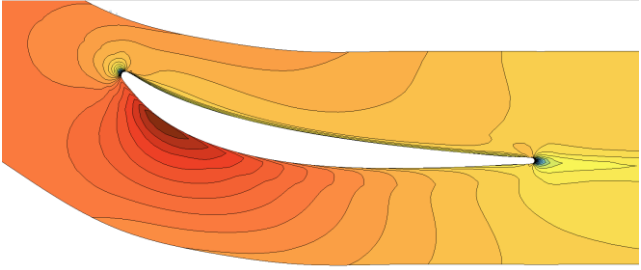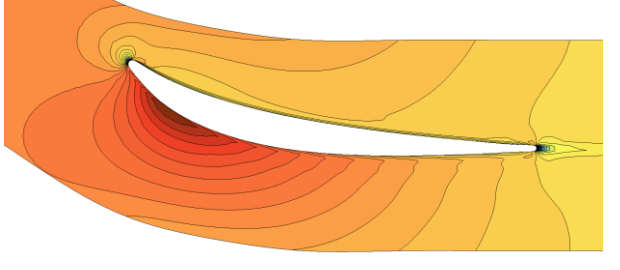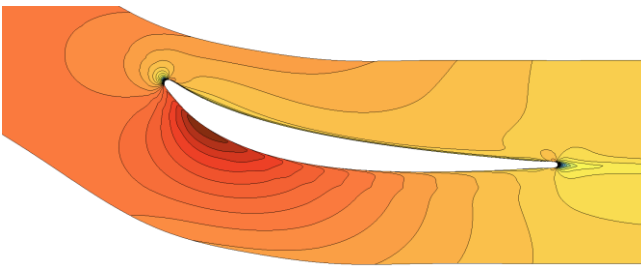
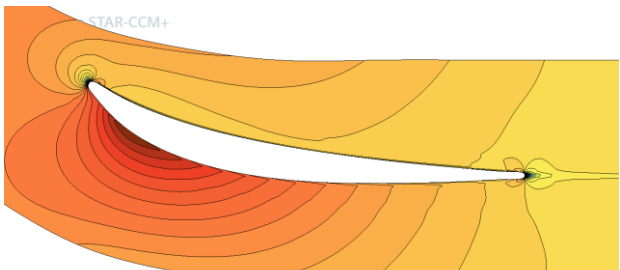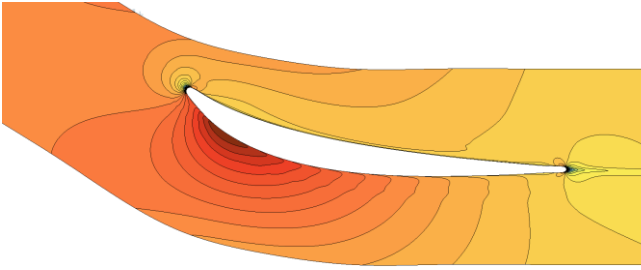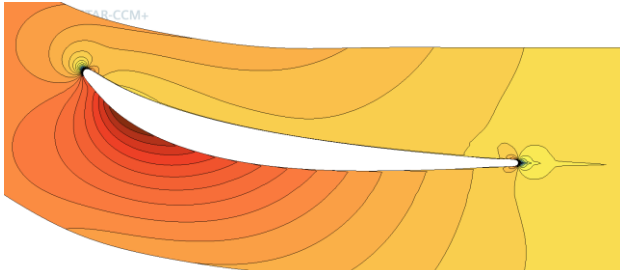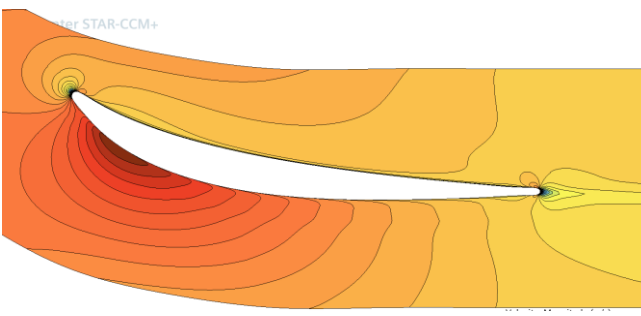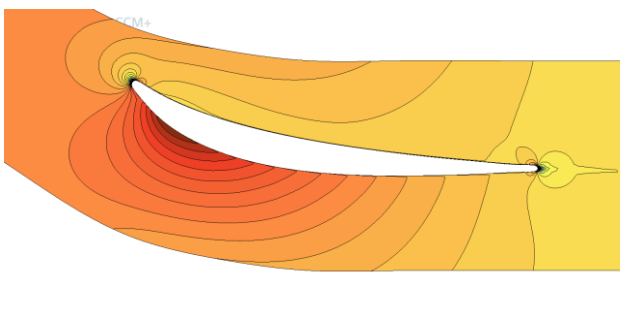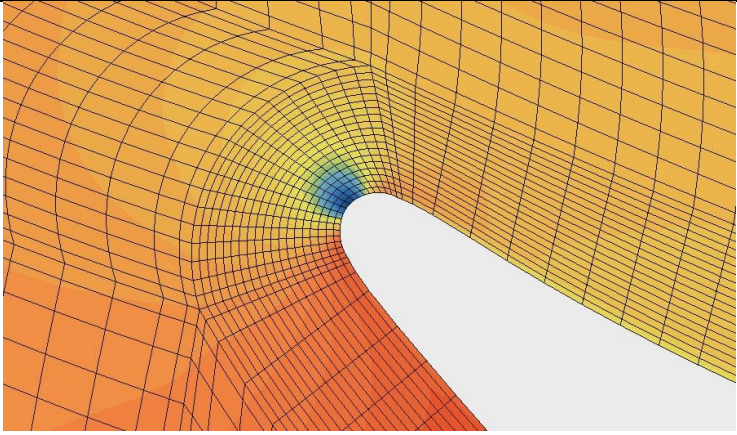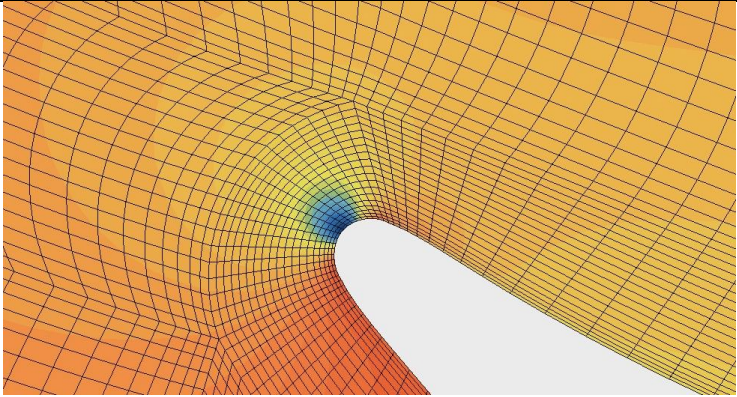| Mesh Type	First Order	Second Order
Coarse		
Medium		
Fine		
Other		
Legend		

Table 2 - Mesh around the leading edge of the second order, medium and other meshes.

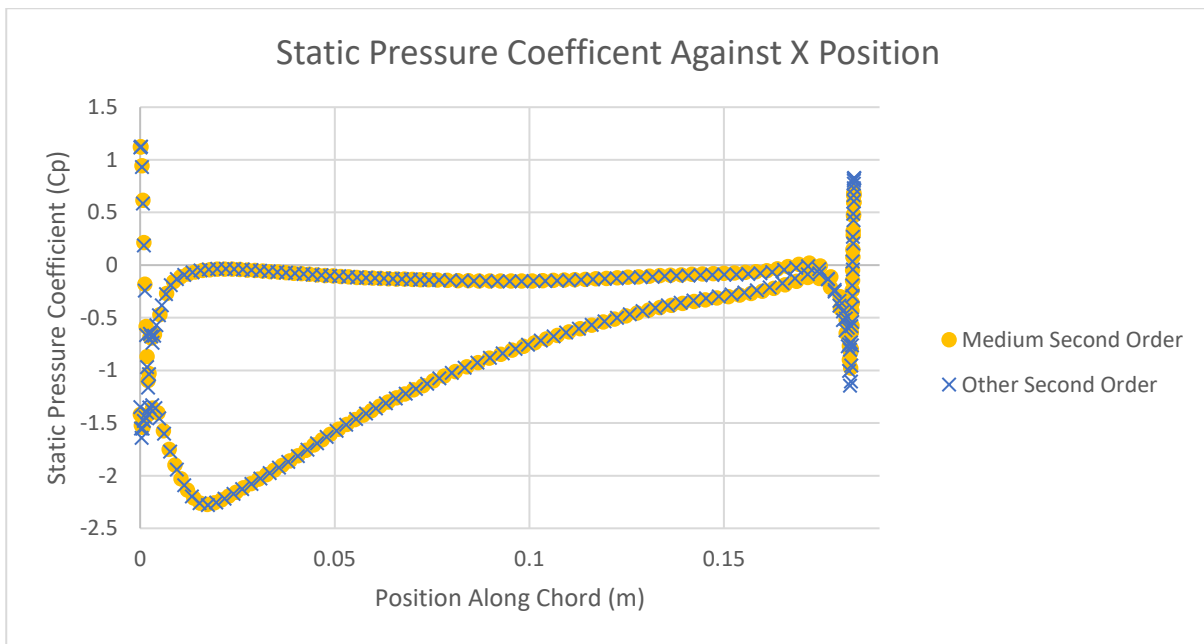| Mesh type	
Medium	
Other	
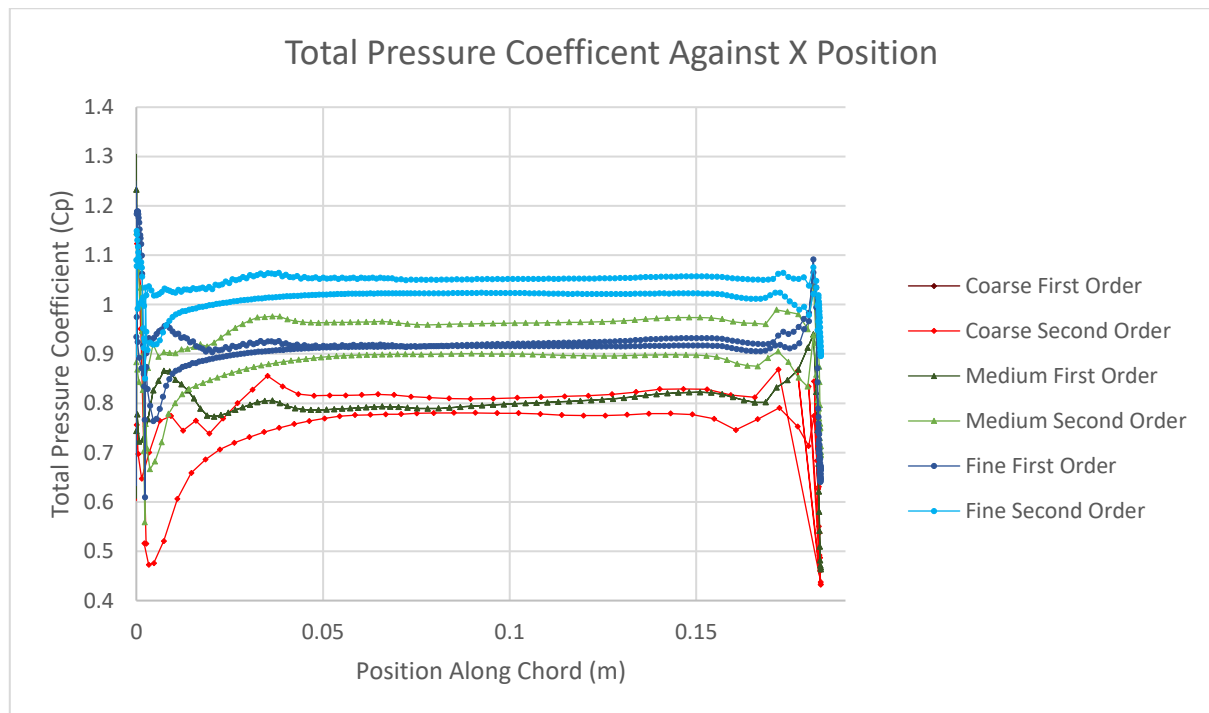
Graph 1 - Total pressure coefficient along the blade for all sequence mesh and order types.
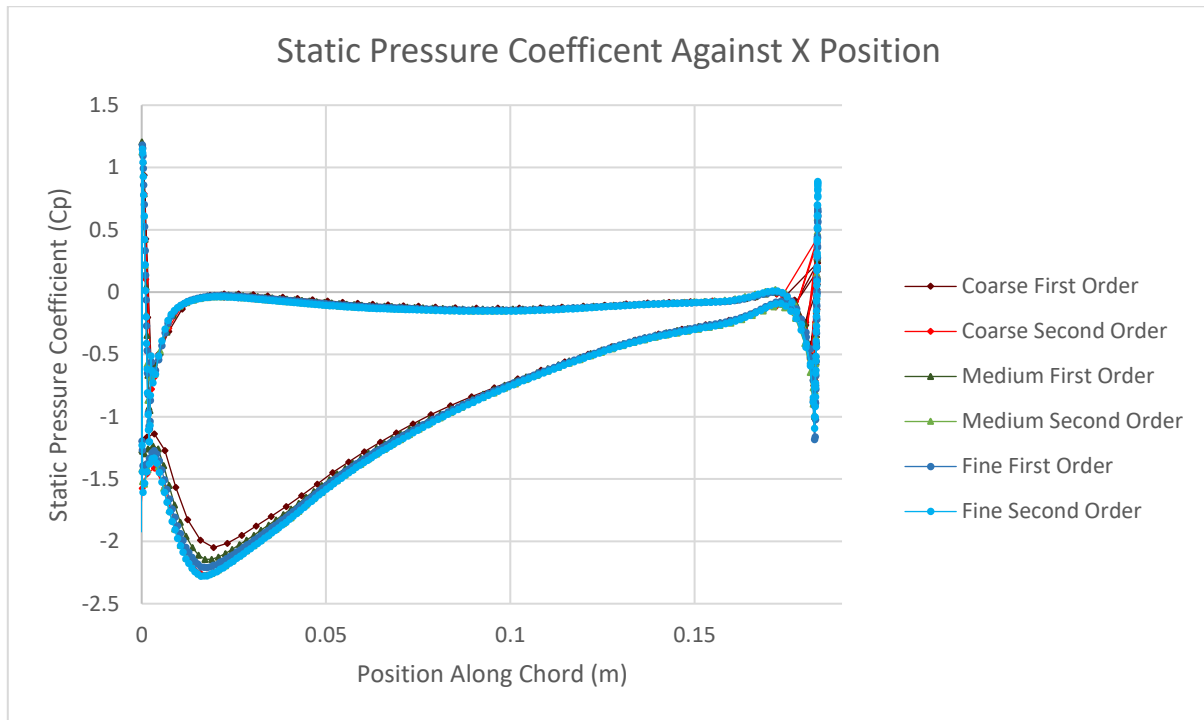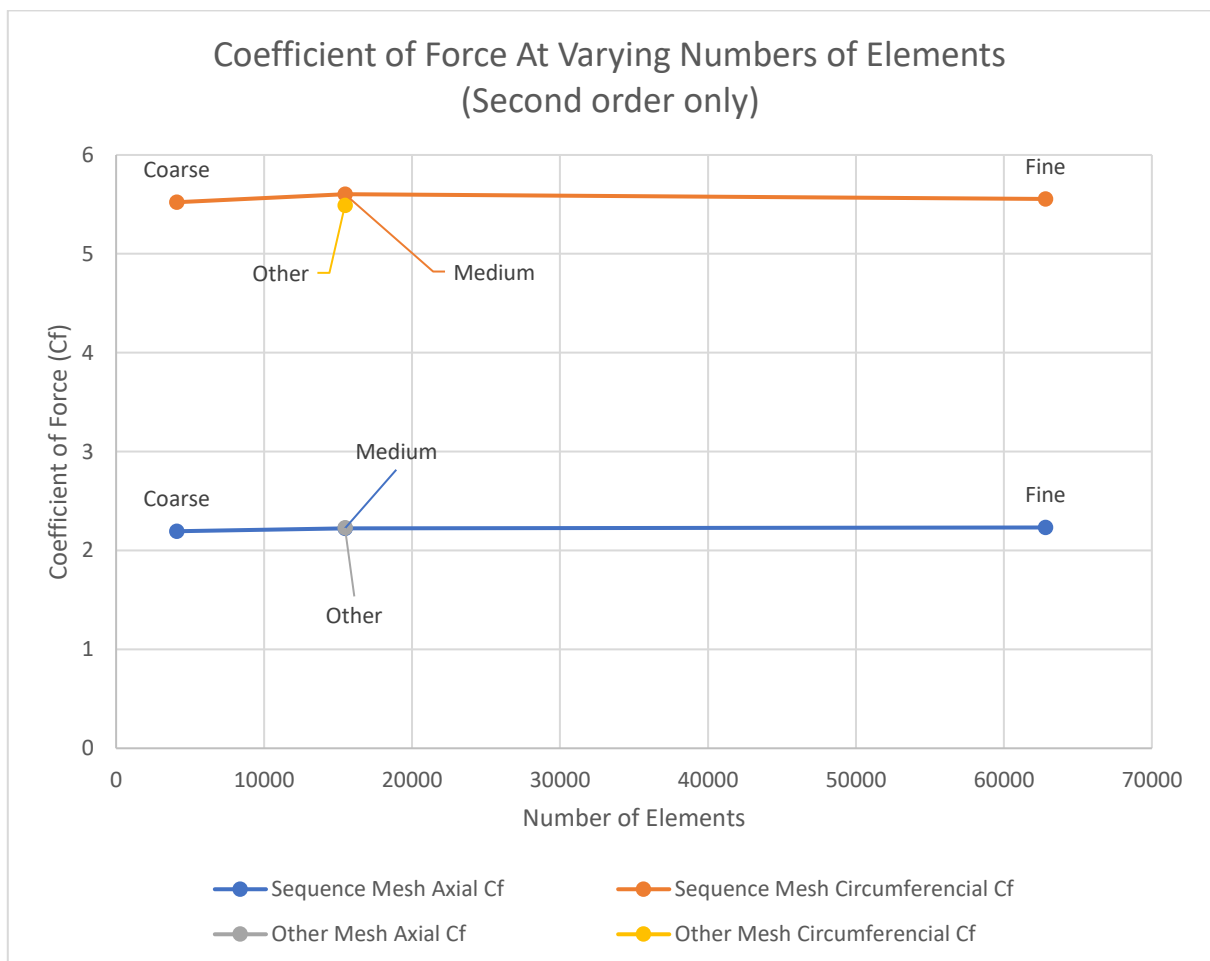
Graph 2 - Static pressure coefficient along the blade for all sequence mesh and order types.
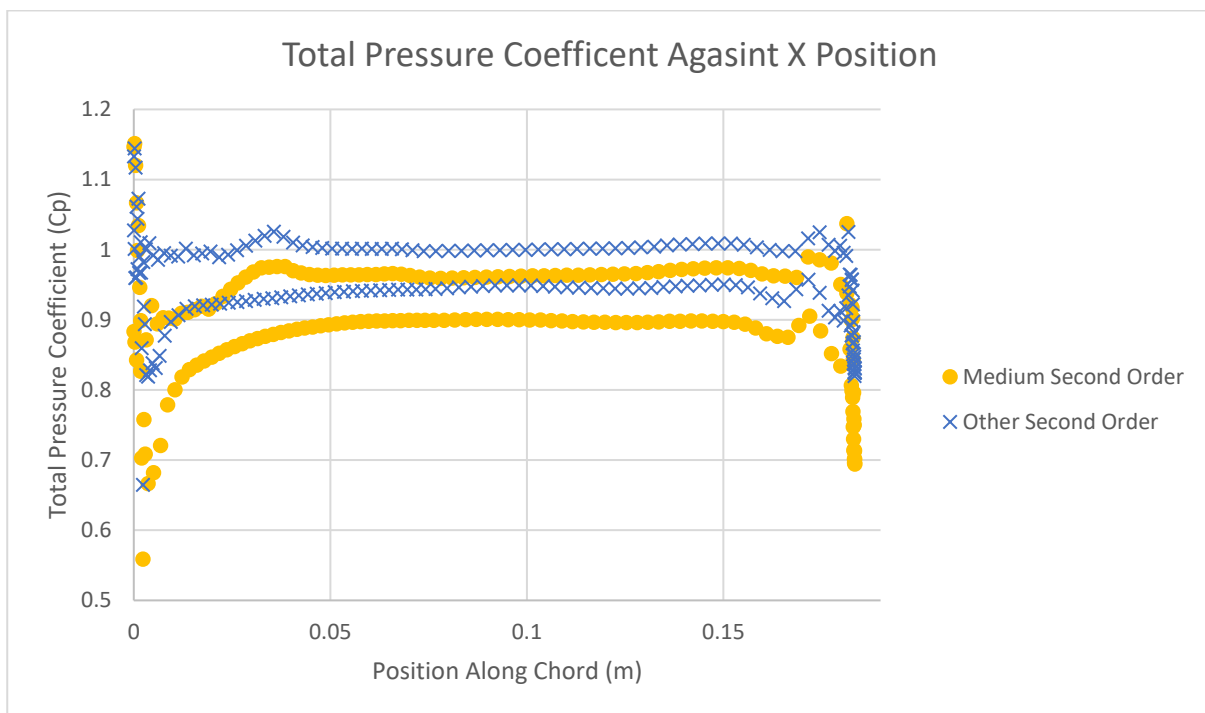
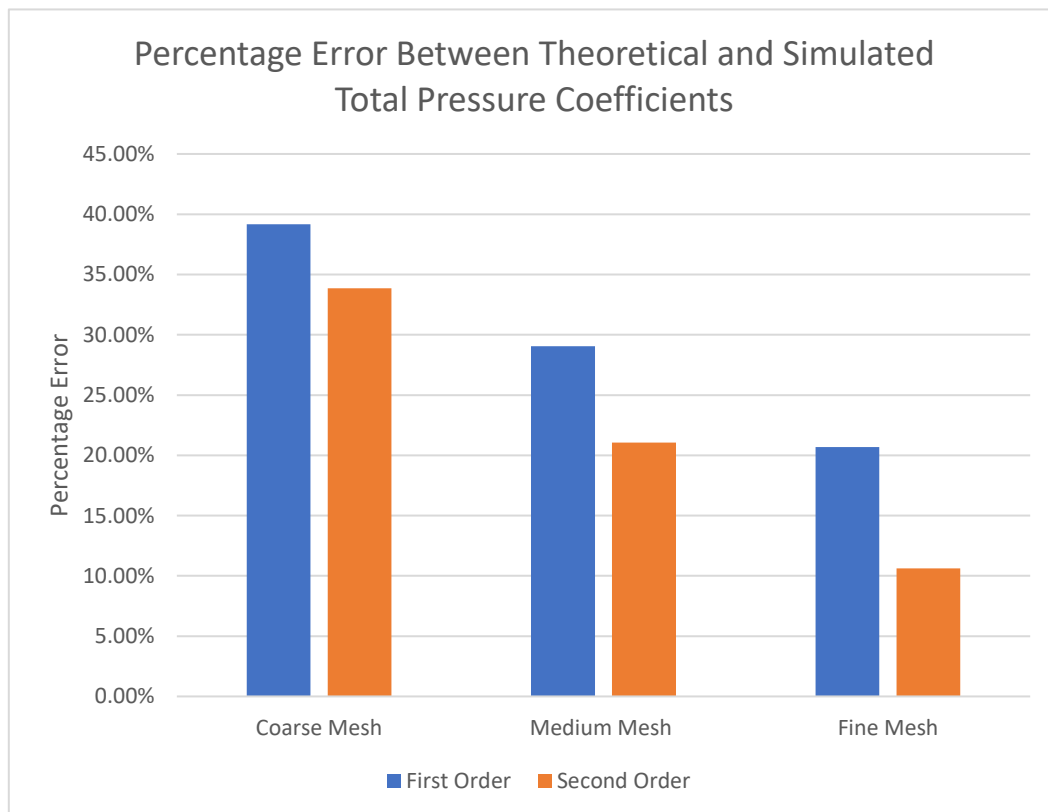*Graph 3 - Total pressure coefficient along the blade for second order medium and other meshes.*

Graph 4 - Static pressure coefficient along the blade for second order medium and other meshes.


Graph 5 - Coefficient of force against number of elements.

Table 3 - Percentage Error Between Theoretical and Average Simulated Total Pressure Coefficients.

		Coarse Mesh	Medium Mesh	Fine Mesh
First Order	**Average Experimental Cp**	0.697264065	0.813062016	0.909046
	% Error	39.17%	29.06%	20.69%
Second Order	**Average Experimental Cp**	0.758128445	0.904689857	1.0244875
	% Error	33.86%	21.07%	10.62%

Graph 6- Percentage Error Between Theoretical and Simulated Total Pressure Coefficients.
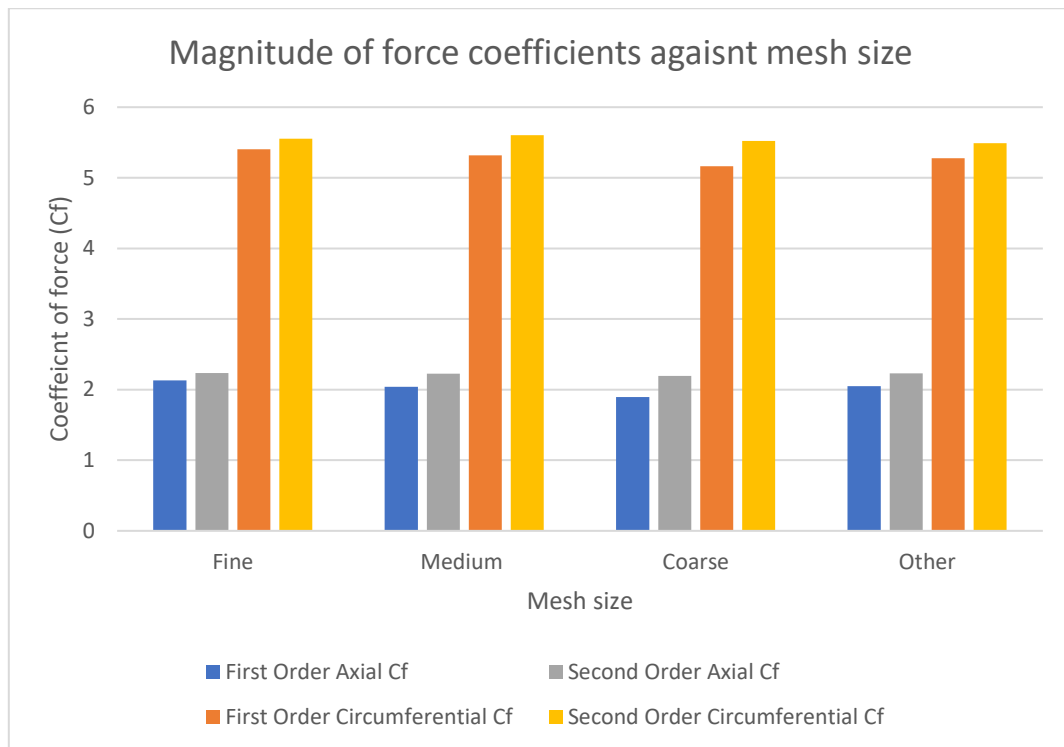
Graph 7 - Magnitude of force coefficient for each mesh size and order of accuracy.